AD-A179 358 DIRECT NUMERICAL SIMULATIONS OF AN UNPREMIXED TURBULENT 1/1
JET FLAME(U) FLOW RESEARCH CO KENT WA APPLIED MECHANICS
DIV P GIVI ET AL. MAR 87 FLOW-TR-401 AFOSR-TR-87-0460
UNCLASSIFIED F49620-85-C-0067 F/G 21/2 NL

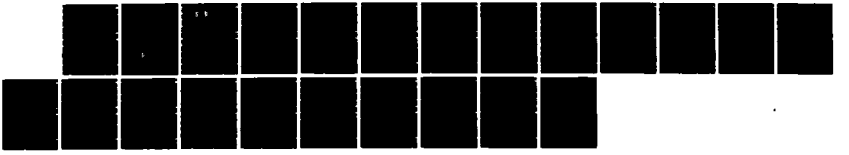

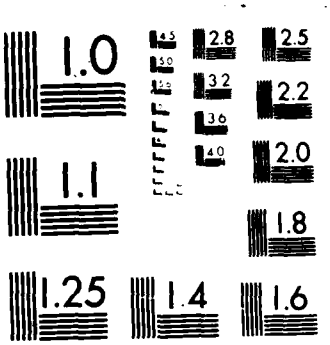

(2)

Flow Technical Report No. 401

AFOSR-TR- 87-0460

DTIC FILE COPY

AD-A179 358

DIRECT NUMERICAL SIMULATIONS OF AN UNPREMIXED TURBULENT JET FLAME

Approved for public release;
distribution unlimited.

Annual Report

(February 16, 1986 - February 16, 1987)

by

P. Givi, W.-H. Jou and

R. W. Metcalfe

March 1987

FLOW RESEARCH COMPANY
Applied Mechanics Division
21414-68th Avenue South
Kent, Washington 98032
(206) 872-8500

Unclassified
SECURITY CLASSIFICATION OF THIS PAGE

AD-A179 357

DTIC ELECTE APR 22 1987 S D

REPORT DOCUMENTATION PAGE

1a. REPORT SECURITY CLASSIFICATION: Unclassified	1b. RESTRICTIVE MARKINGS: None
2a. SECURITY CLASSIFICATION AUTHORITY:	3. DISTRIBUTION/AVAILABILITY OF REPORT: Distribution unlimited; approved for public release
2b. DECLASSIFICATION/DOWNGRADING SCHEDULE:	
4. PERFORMING ORGANIZATION REPORT NUMBER(S): Flow Research Report No. 401	5. MONITORING ORGANIZATION REPORT NUMBER(S): AFOSR-TR- 87-0460
6a. NAME OF PERFORMING ORGANIZATION: Flow Industries, Inc. / 6b. OFFICE SYMBOL (If applicable):	7a. NAME OF MONITORING ORGANIZATION: Air Force Office of Scientific Research
6c. ADDRESS (City, State and ZIP Code): 21414-68th Avenue South, Kent, WA 98032	7b. ADDRESS (City, State and ZIP Code): Bolling AFB DC 20332-6448
8a. NAME OF FUNDING/SPONSORING ORGANIZATION: Air Force Office of Sci. Res. / 8b. OFFICE SYMBOL (If applicable): AFOSR/NA	9. PROCUREMENT INSTRUMENT IDENTIFICATION NUMBER: F49620-85-C-0067
8c. ADDRESS (City, State and ZIP Code): Bolling AFB DC 20332-6448	10. SOURCE OF FUNDING NOS.

PROGRAM ELEMENT NO.	PROJECT NO.	TASK NO.	WORK UNIT NO
61102F	2308	A2	

11. TITLE (Include Security Classification): Direct Numerical Simulations of an Unpremixed Turbulent Jet Flame(U)

12. PERSONAL AUTHOR(S): P. Givi, W.-H. Jou, and R. W. Metcalfe

13a. TYPE OF REPORT	13b. TIME COVERED	14. DATE OF REPORT (Yr., Mo., Day)	15. PAGE COUNT
Annual	FROM 2/86 TO 2/87	March 1987	18

16. SUPPLEMENTARY NOTATION:

17. COSATI CODES			18. SUBJECT TERMS (Continue on reverse if necessary and identify by block number)
FIELD	GROUP	SUB. GR.	
21	01		
21	02		

19. ABSTRACT (Continue on reverse if necessary and identify by block number)

A hybrid spectral-finite element computer code has been developed for direct numerical simulations of spatially developing three-dimensional turbulent flows under the influence of finite-rate chemical reactions. The spectral element method combines the generality of the finite element methods with the accuracy of the spectral techniques, which permits accurate simulations of flows with realistic boundary conditions.

The finite elements are located in the direction of spatial development of the flow, and each element is composed of discrete Chebyshev collocation points. Pseudospectral methods using Fourier transforms have been used in the other two directions of the flow. The code has been constructed in a manner that allows the number of data buffering operations to be easily optimized for the memory capabilities of the computer.

The algorithm has been tested by comparing the numerical results to some known analytical results. Large-scale simulations are the subject of the present research.

20. DISTRIBUTION/AVAILABILITY OF ABSTRACT	21. ABSTRACT SECURITY CLASSIFICATION
UNCLASSIFIED/UNLIMITED ☒ SAME AS RPT. ☐ DTIC USERS ☐	Unclassified

22a. NAME OF RESPONSIBLE INDIVIDUAL	22b. TELEPHONE NUMBER (Include Area Code)	22c. OFFICE SYMBOL
Julian M. Tishkoff	(202)767-4935	AFOSR/NA

DD FORM 1473, 83 APR — EDITION OF 1 JAN 73 IS OBSOLETE.

Unclassified
SECURITY CLASSIFICATION OF THIS PAGE

TABLE OF CONTENTS

87-4-21-211

OBJECTIVES

The objectives of this work are to develop and implement numerical techniques that will enable us to perform simulations of spatially evolving phenomena. In particular, we are interested in studying the phenomenon of turbulent diffusion flame lift-off.

The flame lift-off phenomenon occurs when the speed of the fuel jet exceeds a certain value. The flame detaches from the exit and is stabilized at a certain distance downstream. Different mechanisms have been proposed to explain the lift-off phenomenon. Generally, it is believed that the phenomenon is similar to that in premixed gas combustion (Brzustowski, 1980; Gunther et al., 1981). At the jet exit, the velocity of the fluid in the mixing layer is higher than the flame propagation speed. The flame cannot be stabilized at that location. As the mixing proceeds, the velocity of the fluid in the mixing layer, where the species ratio roughly becomes stoichiometric, decreases to the flame speed. The flame is stabilized at that position. This model assumes that the mixing of the fuel and the oxidizer as predicted by the nonreacting turbulence model reaches the molecular level everywhere in the mixing layer. Direct numerical simulations of a reacting mixing layer (Riley et al., 1986) indicated that this may not be the case.

Another model was suggested by Peters and Williams (1983). They proposed that, in a turbulent mixing layer, the turbulent eddies produce highly stretched and contorted sheets across which molecular diffusion of species occurs. Combustion appears as laminar flamelets on these sheets. Based on the theory that a laminar flame will extinguish itself if the strain rate is sufficiently high that the local reduced Damkohler number is lower than a critical value (Linan, 1974), Peters and Williams predicted that the strain rate near the exit of the jet is too high for the flame to exist. As the mixing layer grows, the strain rate is reduced to a sufficiently low level that a flame can be sustained. They proceeded to estimate the strain rate in the mixing layer. Through a statistical theory that predicts disruption of a continuous sheet due to "holes" on the sheet, they were able to obtain quantitative results for lift-off distance. Their theoretical predictions of lift-off heights are of the right "order of magnitude" for limited methane flame data.

The results of Peters and Williams, based on simple turbulence models, are encouraging. However, a detailed numerical simulation of the interaction between fluid dynamical and combustion processes that occur in diffusion flames would be invaluable to further our understanding of the physics.

Direct numerical simulations consist of accurately solving appropriate convection-diffusion-reaction transport equations by means of very accurate numerical algorithms so that no turbulence modeling is required. The direct numerical simulation technique has recently been successfully applied to chemically reacting flows. Riley et al. (1986) considered the three-dimensional temporally growing mixing layer under the simplest possible assumption of a constant-rate chemical reaction with no heat release. The main contribution of this work is the understanding of the effects of three-dimensional mixing and diffusion of the species on the chemical reaction. McMurtry et al. (1985) considered the effects of chemical heat release and the resulting density variation on the fluid motion for a two-dimensional mixing layer. The fluid dynamics and the chemical reaction are truly coupled in this work, and the interplay between the two are discussed. However, the assumption of a constant chemical reaction is still employed. We intend to extend the simulations to study the local quenching and the lift-off of a diffusion flame. The existing methods must be modified to include (1) a temperature-dependent chemical reaction rate and (2) a spatially developing flow.

STATUS OF THE RESEARCH

In the first year of this research, we focused on an initial understanding of the physical aspects of the problem through simulations of two-dimensional flows. During the second year, we mainly concentrated on construction of an accurate three-dimensional numerical code.

In the first year, we examined the effects of large coherent structures in two-dimensional, unpremixed chemically reacting mixing layers under both temporally evolving and spatially developing assumptions. The results were reported in detail by Givi et al. (1986) and are only summarized here.

(1) In a two-dimensional temporally evolving mixing layer, a temperature-dependent chemical reaction was incorporated into a computer code that uses pseudospectral numerical methods. The nonequilibrium effects leading to the local quenching of a diffusion flame were investigated. The results indicated that the most important parameter to be considered for flame extinction is the local instantaneous scalar dissipation rate conditioned at the scalar stoichiometric value. At locations where this value is increased beyond a critical value, the local temperature decreases and the instantaneous reaction rate drops to zero, leading to the local quenching of the flame. This work was published by Givi et al. (1987).

(2) For the purpose of simulating spatially developing flows, a two-dimensional hybrid pseudospectral-finite difference code was developed. The resulting code was used for the simulation of the pre-transitional region of a laboratory mixing layer. The asymmetric nature of the mixing process was numerically simulated and the "preferred" mixed concentration value (Masutani and Bowman, 1987) was numerically calculated by constructing the profiles of the probability density function of a passive scalar quantity across the shear layer. The results of this simulation were also used to explain the shortcomings associated with turbulence models using gradient diffusion approximations to model the turbulent flux of the pdf, such as the one used previously by Givi et al. (1985). This work was published by Givi and Jou (1987).

To understand the exact mechanism of the lift-off in turbulent flames, direct numerical simulations of three-dimensional, spatially evolving flows under the influence of finite-rate chemical reactions are required. For this

purpose, during the second year we have concentrated on constructing an accurate numerical code for the simulations of such flows. In this code, the governing equations describing the hydrodynamic variables (velocities and pressure) and scalar quantities (such as concentrations and mixture temperature) are solved by means of a spectral element method. This method combines the versatility of finite element techniques with the accuracy of spectral methods in a more flexible manner than that found in either technique alone (Patera, 1984). This approach permits arbitrary boundary conditions, therefore allowing us to simulate spatially evolving flows more accurately.

The geometrical configuration of the type of the flow to be considered is presented in Fig. 1. The flow is three-dimensional and evolves spatially in the streamwise (x) direction. An explanation of the spectral element algorithm is given in Appendix I, and a detailed explanation of the computer code is Given by Givi and Israeli (1987). Here, we summarize the properties of the technique.

(1) The streamwise direction is divided into (NB) number of blocks. At any time during computation only one block is in fast memory core while the other blocks are in secondary storage (such as the SSD or disk) and can be accessed when required. Division of the domain in this manner has been done to ensure portability of the code for different computers, especially those with builted fast memory. For example, on a CRAY-2 computer (with 256M words of memory) NB can be set equal to 1 with a minimum amount of data buffering, and the values of NB can be increased to accommodate machines with smaller memories.

(2) Each block is divided into NE number of elements, and each element consists of NI number of Chebyshev collocation spectral modes in the streamwise direction. This division has the advantage that, by increasing the number of elements (increasing NE) for better resolution, fewer Chebyshev modes (NI) are required. Therefore, the distance between two neighboring Chebyshev points, particularly near the boundaries of the elements, will not be unreasonably small. Thus, the time stepping stability constraints can be reduced.

(3) The flow is assumed periodic in the spanwise direction (z), and impermeable free-slip boundary conditions are employed in the cross-stream direction (y). Pseudospectral methods with Fourier transforms are used in these directions.

(4) The transport equations are solved in Fourier space, after the Fourier transformation of the variables in the y and z directions. The evaluation of the nonlinear convection terms, however, is performed in physical space. A second-order-accurate Adams-Bashforth technique (Roach, 1972) is employed for the time discretization.

The hybrid spectral element algorithm used in the streamwise direction has the advantage that the accuracy of spectral methods is maintained in the flow direction. In most previous work, the streamwise derivatives were usually discretized by second-order-accurate finite difference methods, where the convective terms were approximated by an upwind difference scheme (Givi and Jou, 1987; Lowery et al., 1987). Second-order central differencing requires a maximum cell Reynolds (Peclet) number of 2 (Roach, 1972), which can require an excessive number of grid points in the x-direction. The upwind scheme results in an improvement of the capability in resolving sharp gradients for moderate Reynolds number flow simulations. However, it results in the addition of an artificial numerical viscosity to the fluid viscosity, which is not desirable, particularly in diffusion flame simulations. The implementation of the spectral element methods in the streamwise direction will allow us to simulate flows with higher Reynolds numbers accurately without the addition of any artificial viscosity.

We have just completed the construction and debugging of the code. The finite element matrices and the Chebyshev discretization routines are accurately constructed. Some simple problems with known analytical solutions have been used as test problems. The results of preliminary tests using spectral element methods show excellent agreement with the analytical solutions (see Appendix I).

After validating the code by comparison of the data with known analytical results, simulations of a laminar three-dimensional plane jet were performed. In Fig. 2 we present contour plots of the instantaneous axial velocity of the jet in a x-y plane. The figure corresponds to a time when the fluid has swept the computational domain once. A very coarse grid was chosen (16**3) for the purpose of demonstration. As shown on the figure, the linear growth of the laminar jet is well predicted. The computational time for this simulation was about 0.61 sec/time step on a CRAY-XMP, which is very encouraging and indicates that higher resolution simulations can be performed.

CURRENT ACTIVITIES

We are presently starting the simulations of turbulent diffusion flames with finite rate chemical reactions. The resulting code will be used to study a three-dimensional turbulent flow field in a spatially evolving jet and the structure of the "holes" on the flame sheet. Variable density effects caused by the heat release will then be added to the code at a later stage.

PUBLICATIONS

The following written manuscripts have resulted from our efforts during the second year:

(1) Givi, P., and Jou, W.-H., "Mixing and Chemical Reactions in a Spatially Developing Mixing Layer," accepted for publication in Journal of Non-Equilibrium Thermodynamics, to appear (1987); also presented at Spring Technical Meeting of The Combustion Institute, Central States Section, Cleveland, Ohio, May 5-6, 1986.

(2) Givi, P., Jou, W.-H., and Metcalfe, R. W., "Flame Extinction in a Temporally Developing Mixing Layer," Proceedings of the 21st Symposium (International) on Combustion, to appear (1987).

The following paper was in part a result of this work:

(1) McMurtry, P. A., and Givi, P., "Direct Numerical Simulations of Scalar Dissipation in a Turbulent Mixing Layer", SIAM Conference on Numerical Combustion, P. A23, Paper #77, San Francisco, CA, March 9-11 (1987).

INTERACTIONS

In addition to the above-mentioned papers, parts of this work were presented at the following seminars:

(1) Givi, P., "Model Free Simulations of Turbulent Diffusion Flames," Invited Seminar, Graduate Seminar Series, Winter Quarter, Department of Mechanical Engineering, University of Washington, Seattle, WA, February 3, 1987.

(2) Givi, P., "Direct Numerical Simulations of Turbulent Diffusion Jet Flames," Invited Seminar, Fall Seminar Series, Department of Mechanical and Aerospace Engineering, Case-Western Reserve University, Cleveland, Ohio, September 26, 1986.

(3) Givi, P., "Fundamental Studies on Turbulent Combustion and Spray Combustion," ICOMP, NASA Lewis Research Center, Cleveland, Ohio, September 10, 1986.

APPENDIX I

A SUMMARY OF THE SPECTRAL ELEMENT METHOD

APPENDIX I

A SUMMARY OF THE SPECTRAL ELEMENT METHOD

FORMULATION

The geometrical configuration is shown in Fig. 1. The flow evolves spatially in the streamwise direction, x, is periodic in the spanwise direction, z, and impermeable boundary conditions are used in the cross-stream direction, y. For the purpose of demonstration, only the normalized transport equations of the hydrodynamical variables ($\underline{U}$ and P) are considered:

$$\nabla \cdot \underline{U} = 0 \tag{1}$$

$$\frac{\partial \underline{U}}{\partial t} = \underline{U} \times \underline{\Omega} - \nabla P + \frac{1}{Re} \nabla^2 \underline{U} \tag{2}$$

where

P = Dynamic pressure = $p + (1/2)\underline{U} \cdot \underline{U}$

$\underline{\Omega}$ = Vorticity = $\nabla \times \underline{U}$

Re = Reynolds mumber

Employing a second-order Adams-Bashforth scheme for the temporal discretization, we would have:

$$\frac{\underline{U}^* - \underline{U}^n}{\Delta t} = \frac{3}{2} (\underline{U} \times \underline{\Omega})^n - \frac{1}{2} (\underline{U} \times \underline{\Omega})^{n-1} \tag{3}$$

$$\nabla^2 P^* = \frac{1}{\Delta t} (\nabla \cdot \underline{U}^*) \tag{4}$$

$$\frac{1}{Re} \nabla^2 \underline{U}^{n+1} - \nabla P^* = \frac{\underline{U}^{n+1} - \underline{U}^*}{\Delta t} \tag{5}$$

where Δt is the computational time increment, and the superscripts n, *, and n+1 refer to the previous, intermediate, and future times, respectively.

Equation (3) constitutes the nonlinear step, and the derivatives on the RHS of this equation can be evaluated by the use of Chebyshev spectral methods (Gottlieb and Orszag, 1977). The cross terms are evaluated in physical space, and the velocities are updated in time by the second-order-accurate Adams-Bashforth scheme.

Equations (4) and (5) constitute the pressure step and the viscous step, respectively. Their numercial simulations can be achieved by finite element methods.

Taking the Fourier transform of Equation (5), we have:

$$\underline{\tilde{U}}^{n+1}_{xx} - \left[(K^2+L^2)+\frac{Re}{\Delta t}\right] \underline{\tilde{U}}^{n+1} = Re\,\widetilde{\nabla P^*} - \frac{Re}{\Delta t}\,\underline{\tilde{U}}^{*} \qquad (6)$$

In this equation, ~ indicates the Fourier domain, K and L are the Fourier wave numbers in the y and z directions, respectively. The subscript x denotes the derivative in the streamwise direction. Following the same procedure for the pressure equation, we have:

$$\tilde{P}^{*}_{xx} - (K^2+L^2)\,\tilde{P}^{*} = \frac{\widetilde{\nabla \cdot V^{*}}}{\Delta t} \qquad (7)$$

Note that Equations (6) and (7) can be written in a generalized form:

$$U_{xx} - \lambda^2 U = f \qquad (8)$$

where λ^2 represents the coeffients of $\tilde{\underline{U}}$ and $\tilde{P}$, and f represents the RHS.

Employing the variational principle equivalent to the solution of Equation (8), we have the following elemental equation:

$$\underline{\underline{Ae}}\ \underline{U} - \lambda^2\ \underline{\underline{Be}}\ \underline{U} = \underline{\underline{Be}}\ \underline{f} \qquad (9)$$

Where $\underline{\underline{Ae}}$ and $\underline{\underline{Be}}$ are (NI+1)x(NI+1) matrices, and NI is the number of intervals in an element and also the degree of the interpolating polynominal. For a given λ^2, we have

$$\underline{\underline{Ce}} = \underline{\underline{Ae}} - \lambda^2\ \underline{\underline{Be}} \qquad (10)$$

Therefore,

$$\underline{\underline{Ce}}\ \underline{U} = \underline{\underline{Be}}\ \underline{f} = \underline{R} \tag{11}$$

Assume $\underline{U}$ and $\underline{R}$ are decomposed as shown in Fig. 3:

$$\underline{U}^T = \left[U^f,\ \underline{U}^I,\ U^L \right] \tag{12}$$

$$\underline{R}^T = \left[R^f,\ \underline{R}^I,\ R^L \right] \tag{13}$$

where the subscripts f, I and L indicate the first element, the interior elements, and the last element, respectively.

Also, let us decompose the matrix $\underline{\underline{Ce}}$ as follows:

$$\underline{\underline{Ce}} = \left[\begin{array}{c|c|c} De & \underline{RF}^T & Be \\ \hline \underline{RF} & \underline{\underline{AI}} & \underline{RL} \\ \hline Be & \underline{RL}^T & De \end{array}\right] \tag{14}$$

Therefore, we have the elemental equation:

$$\left|\begin{array}{c|c|c} De & \underline{RF}^T & Be \\ \hline \underline{RF} & \underline{\underline{AI}} & \underline{RL} \\ \hline Be & \underline{RL}^T & De \end{array}\right| \left|\begin{array}{c} U^f \\ \hline \underline{U}^I \\ \hline U^L \end{array}\right| = \left|\begin{array}{c} R^f \\ \hline \underline{R}^I \\ \hline U^L \end{array}\right| \tag{15}$$

Solving for the interior elements, $\underline{U}$, we have:

$$\underline{U}^I = (\underline{\underline{AI}})^{-1} \left[\underline{R}^I - \underline{RF}\, U^f - \underline{RL}\, U^L \right] \tag{16}$$

and denoting $(\underline{\underline{AI}})^{-1}$ by $\underline{\underline{A}}$, we have:

$$\underline{U}^I = \underline{\underline{A}}\, \underline{R}^I - U^f\, \underline{\underline{A}}\, \underline{RF} - U^L\, \underline{\underline{A}}\, \underline{RL} \tag{17}$$

Equation (17) gives the values of the internal nodes in terms of the boundary nodes (static condensation).

Now, assuming the coefficients of the matrices are identical for all the elements, by direct summation, we have:

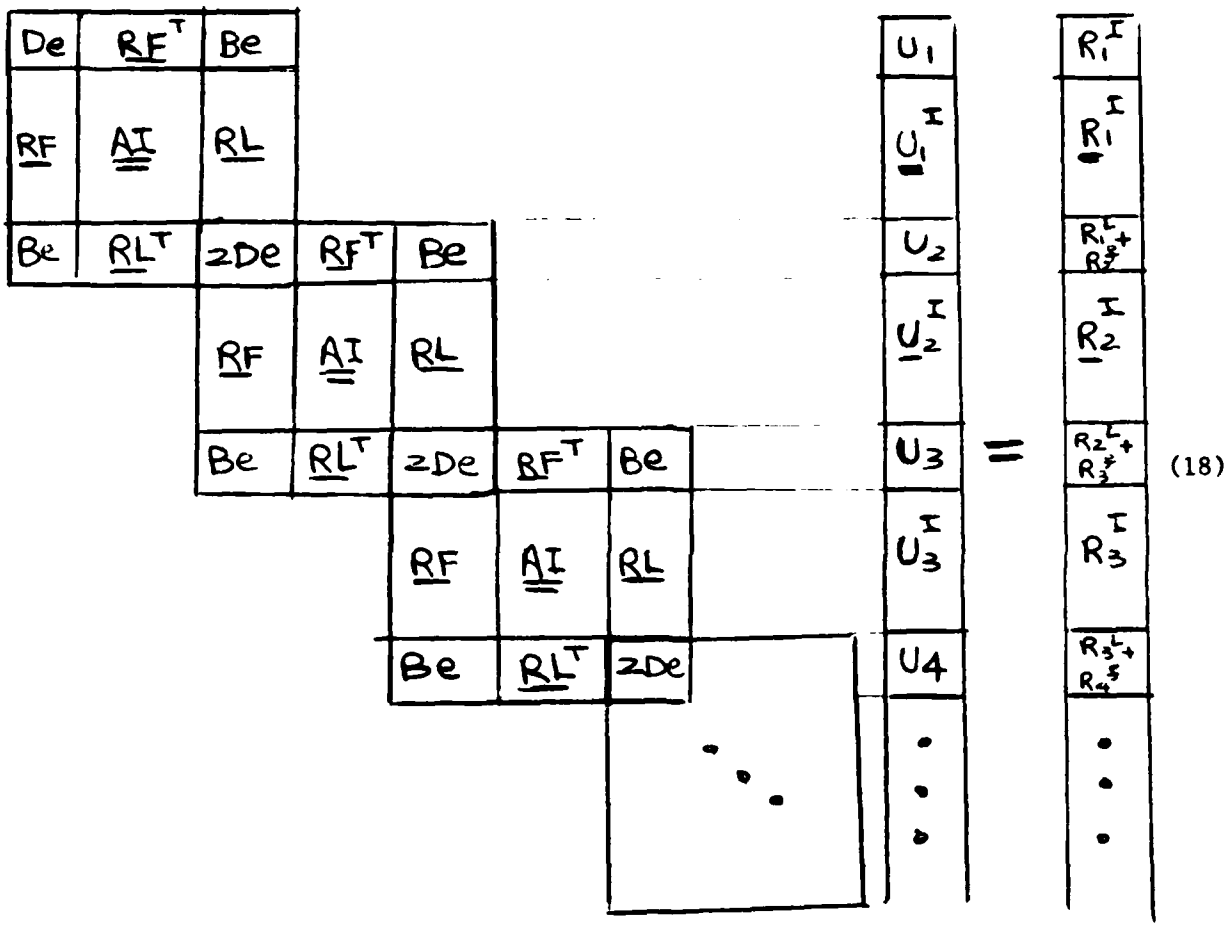

(18)

Consider the first internal equation:

$$Be\,U_1 + \underline{RL}\,\underline{U}_1^I + 2De\,U_2 + \underline{RF}\,\underline{U}_2^I + Be\,U_3 = R_1^L + R_2^F \qquad (19)$$

But, from Equation (17):

$$\underline{U}_1^I = \underline{\underline{A}}\,(\underline{R}_1^I - U_1\,\underline{RF} - U_2\,\underline{RL}) \qquad (20)$$

$$\underline{U}_2^I = \underline{\underline{A}}\,(\underline{R}_2^I - U_2\,\underline{RF} - U_3\,\underline{RL}) \qquad (21)$$

Substituing Equations (20) and (21) in (19), we have:

$$(Be - \underline{RL}\,\underline{\underline{A}}\,\underline{RF})\,U_1 + (2De - \underline{RL}\,\underline{\underline{A}}\,\underline{RF} - \underline{RF}\,\underline{\underline{A}}\,\underline{RL})\,U_2 + (Be - \underline{RF}\,\underline{\underline{A}}\,\underline{RL})\,U_3 = -\underline{RL}\,\underline{\underline{A}}\,\underline{R}_1^I + R_1^L + R_2^F - \underline{RF}\,\underline{\underline{A}}\,\underline{R}_2^I \qquad (22)$$

Equation (22) can be generalized by substituting

$1 \rightarrow j-1$

$2 \rightarrow j$

$3 \rightarrow j+1$

$$(Be - \underline{RL}\,\underline{\underline{A}}\,\underline{RF})\,U_{j-1} + (2De - \underline{RL}\,\underline{\underline{A}}\,\underline{RF} - \underline{RF}\,\underline{\underline{A}}\,\underline{RL})\,U_j + (Be - \underline{RF}\,\underline{\underline{A}}\,\underline{RL})\,U_{j+1} = -\underline{RL}\,\underline{\underline{A}}\,\underline{R}_{j-1}^I + R_{j-1}^L + R_j^F - \underline{RF}\,\underline{\underline{A}}\,\underline{R}_j^I \qquad (23)$$

Note that Equation (23) forms a tridiagonal system of equations that can be solved easily when the values at the interior planes are known.

TEST PROBLEM

To test the viscous solver, the following example is considered:

$$U_{xx} - A^2 U = 0$$

$$U(x=0) = 1 \qquad (24)$$

$$U(x=L) = 0$$

The exact solution of this equation is:

$$U = 1 - X/L \quad \text{if} \quad A = 0$$

$$U = \frac{\text{Sinh}\left[AL\left(1-\frac{x}{L}\right)\right]}{\text{Sinh}\,(AL)} \quad \text{if} \quad A \neq 0 \qquad (25)$$

Equation (24) was solved by the spectral element technique with three elements (NE = 3) and two Chebyshev interpolation points within each element (a total of 7 points in the x direction).

In Fig. 4, the results of the numerical solution are compared with the analytical results. As can be seen, the agreement is excellent.

REFERENCES

Brzustowski, T. A. (1980) Physico-Chemical Hydrodynamics, Vol. 1.

Givi, P., and Israeli, M. (1987) Flow Technical Note, under preparation.

Givi, P., and Jou, W.-H., (1987) accepted for publication in Journal of Non-Equilibrium Thermodynamics, to appear.

Givi, P., Ramos, J. I., and Sirignano, W. A. (1985) Journal of Non-Equilibrium Thermodynamics, Vol. 10, No. 2, pp. 75-104.

Givi, P., Jou, W.-H., and Metcalfe, R. W. (1986) Flow Technical Report No. 369, Annual Report to AFOSR.

Givi, P., Jou, W.-H., and Metcalfe, R. W. (1987) accepted for publication in Proceedings of 21st (Int.) Symposium on Combustion, to appear.

Gottlieb, D., and Orszag, S. A. (1977) Numerical Analysis of Spectral Methods: Theory and Applications, SIAM, Philadelphia, PA.

Gunther, R., Horch, K., and Lenze, B. (1981) First Specialists Meeting (International) of The Combustion Institute, The Combustion Institute, Pittsburgh, pp. 117-122.

Linan, A. (1974) Acta Astronautica, Vol. 1, p. 1007.

Lowery, P. S., Reynolds, W. C., and Mansour, N. N. (1987) AIAA Paper 87-0132.

Masutani, S., and Bowman, C. T. (1987) Journal of Fluid Mechanics, Vol. 172, pp. 93-126.

McMurtry, P. A., Jou, W.-H., Riley, J. J., and Metcalfe, R. W. (1985) AIAA Paper 85-0143. Also AIAA Journal, Vol. 24, No. 6, pp. 962-970.

Patera, A. T. (1984) Journal of Computational Physics, Vol. 54, p. 468.

Peters, N., and Williams, F. A. (1983) AIAA Journal, Vol. 21, pp. 423-429.

Riley, J. J., Metcalfe, R. W., and Orszag, S. A. (1986) Physics of Fluids, Vol. 29, No. 2, pp. 406-422.

Roach, P. (1972) Computational Fluid Dynamics, Hermosa Publishing Company, Albuquerque, New Mexico.

5332R

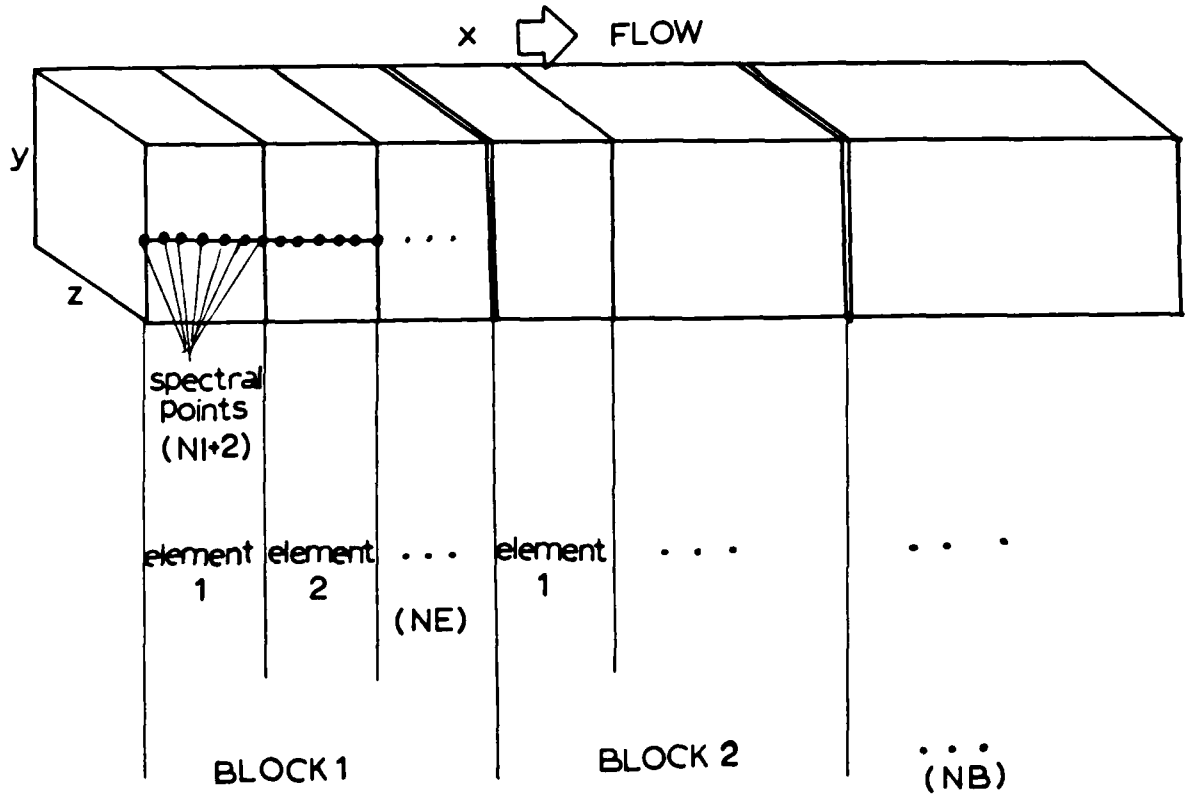
x
FLOW
y
z
spectral
points
(NI+2)
element
1
element
2
(NE)
element
1
BLOCK 1
BLOCK 2
(NB)

Figure 1

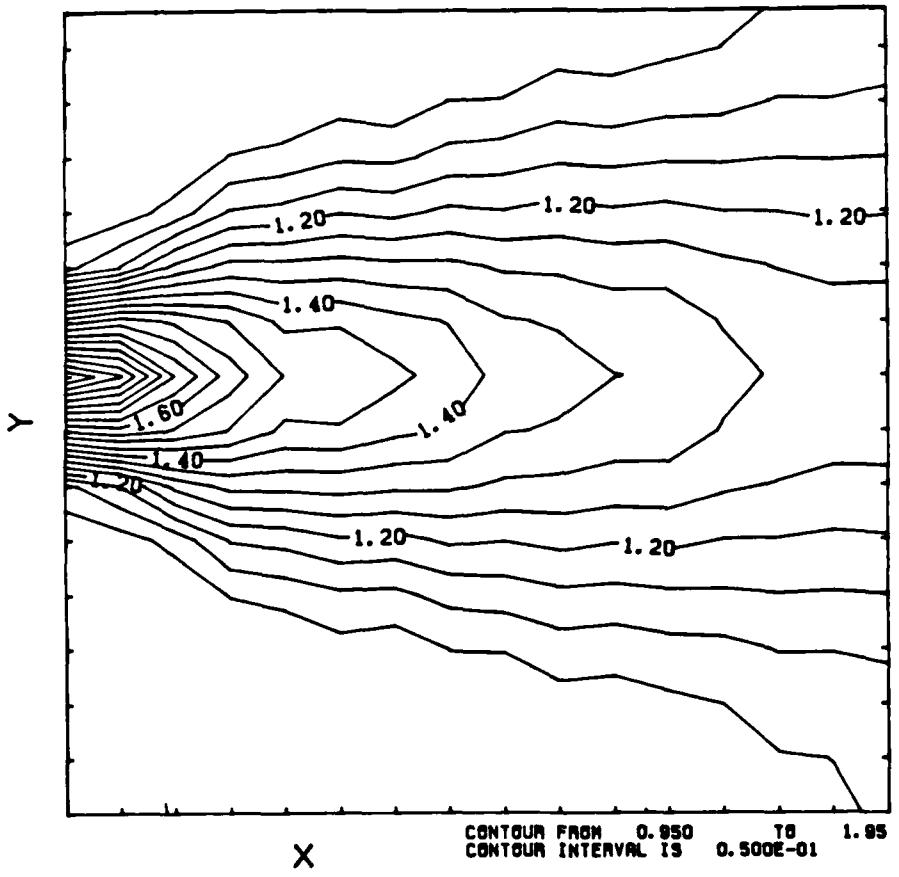
1.20
1.20
1.20
1.40
1.60
1.40
1.40
1.20
1.20
1.20
Y
X
CONTOUR FROM 0.950 TO 1.95
CONTOUR INTERVAL IS 0.500E-01

Figure 2

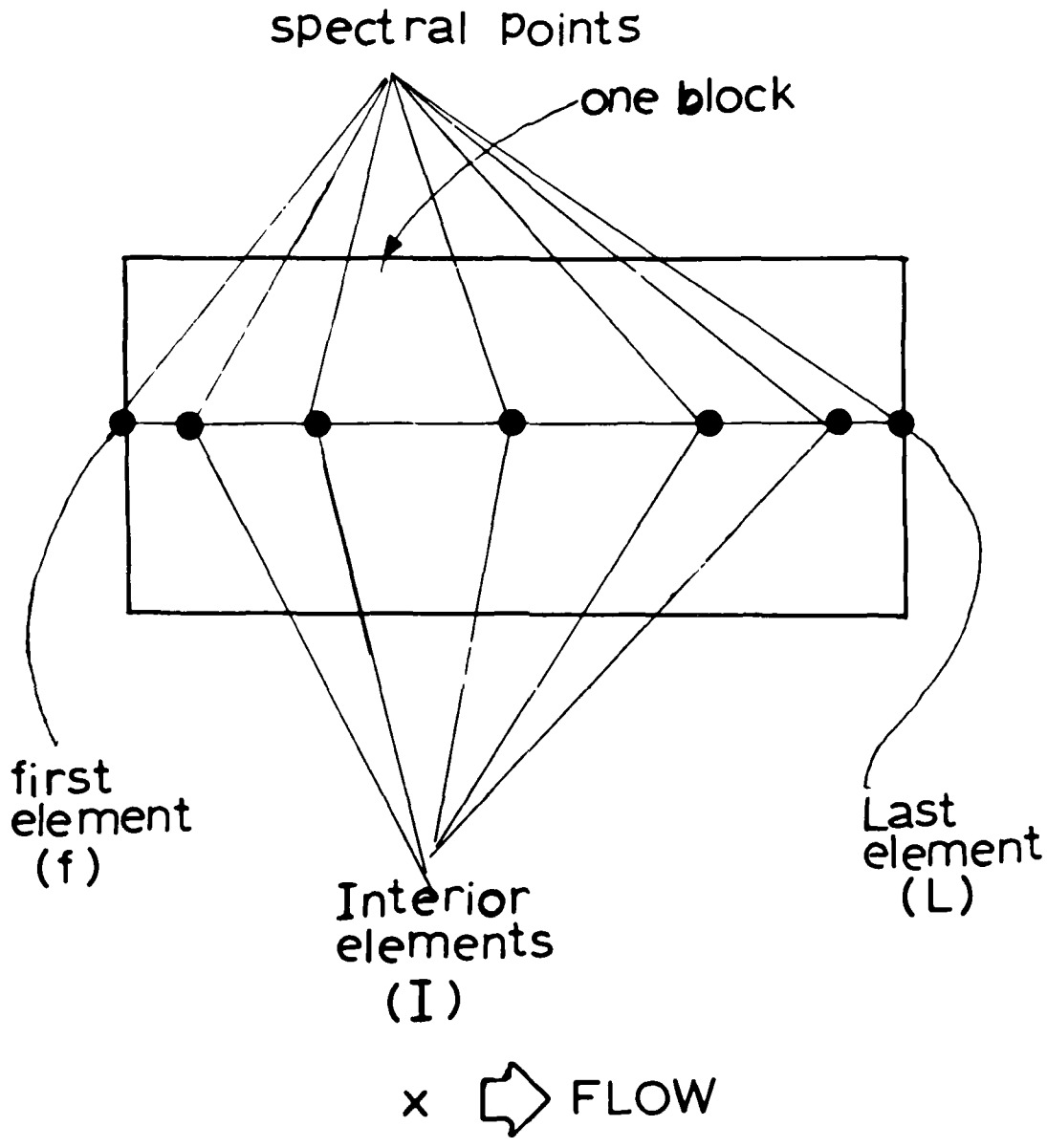
spectral Points
one block
first
element
(f)
Interior
elements
(I)
Last
element
(L)
x
FLOW

Figure 3

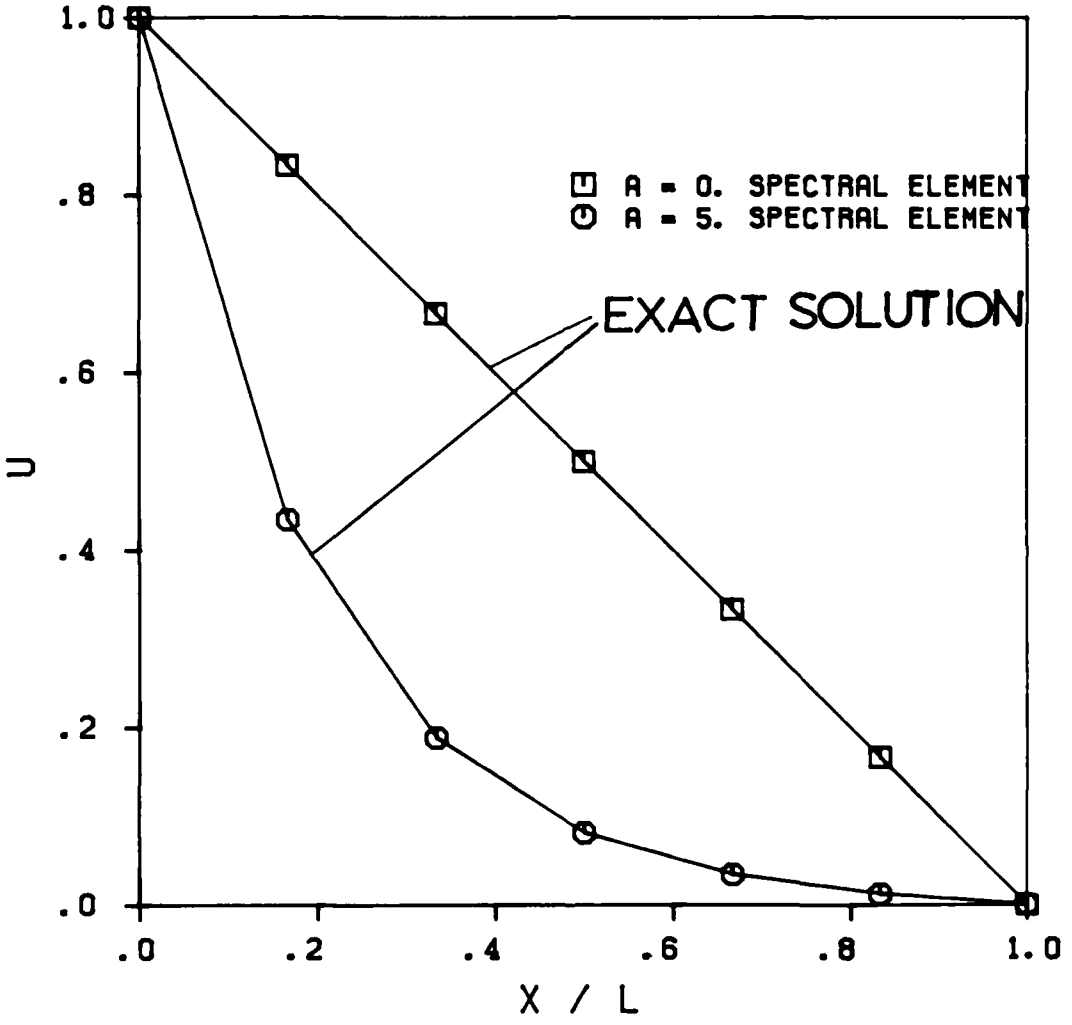
1.0
.8
.6
.4
.2
.0
U
.0
.2
.4
.6
.8
1.0
X / L
A = 0. SPECTRAL ELEMENT
A = 5. SPECTRAL ELEMENT
EXACT SOLUTION

Figure 4

END

5-87

DTIC